

Catalytic Properties of Transition Metal Carbides

I. Preparation and Physical Characterization of Bulk Mixed Carbides of Molybdenum and Tungsten

L. LECLERCQ,¹ M. PROVOST,* H. PASTOR,† J. GRIMBLLOT, A. M. HARDY,‡
L. GENGEMBRE, AND G. LECLERCQ

*Laboratoire de Catalyse Hétérogène et Homogène, UA CNRS No. 402, Université des Sciences et Techniques de Lille Flandres-Artois, 59655 Villeneuve d'Ascq Cédex, France; *Laboratoire de Catalyse Organique, Université de Poitiers, France; †Ugicarb Morgon, B.P. 65X, 38041 Grenoble, France; and ‡Laboratoire de Cristallographie Minérale, Université de Poitiers, France*

Received April 6, 1988; revised December 1, 1988

Unsupported ternary alloys of W and Mo with carbon as mixed carbide catalysts were prepared with various relative compositions of W, Mo, and C in order to be used as reference compounds well characterized for comparison with supported carbides less easy to study by physicochemical methods. X-ray diffraction and XPS were used to study the bulk and the surface structures of the complex phases present. For mixed W, Mo carbides, molybdenum surface enrichment occurs and an attempt to determine the true surface composition has been made. © 1989 Academic Press, Inc.

INTRODUCTION

Metal alloys seem to be most promising materials as catalysts in the immediate future in order to adapt to rapid changes in catalysis in the chemical industry. In particular, new catalytic materials should include metals which are relatively abundant, like W and Mo. Unfortunately, these metals, when alone, are known to be poorly active catalysts in the zero-valent state, whereas they have numerous applications when alloyed with other metals or when sulfided, oxidized, or carbided. Carbiding W and Mo has been proved to be efficient in increasing their activities in hydrocarbon or CO reactions with hydrogen when compared to those of the parent metals (1-4). Although ternary alloys with two metals along with C or N as carbides or nitrides are well documented in metallurgy, they still can be considered new catalytic materials. Moreover, the decline of the use of WC in coating tools, generally linked to the recession in

the steel industry, increases the incentive to find new applications for this carbide, in catalysis for instance.

As pointed out in a review (5) and implemented by recent publications (3, 6-8) two important parameters drastically influence the catalytic activity of carbides:

- the metal-carbon stoichiometry (6, 7).
- the graphitic carbon and oxygen contamination and consequently the activation processes before reactions (3, 8, 9).

Thus, in this paper, we have tried to obtain information as quantitative as possible on the amount of free carbon, superficial oxygen, and carbidic carbon.

Bulk compounds of well-defined structure but with low surface areas are used in this paper (Part I) as reference compounds in a first step toward calibration of X-ray diffraction and XPS instruments. Surface compositions of samples with various contents of W and Mo have been determined by XPS and compared with bulk compositions obtained by chemical analysis. The results of this physical characterization of

¹ To whom correspondence should be addressed.

the catalysts will be correlated with their catalytic activity in cyclohexane dehydrogenation and butane hydrogenolysis in the following paper (Part II).

EXPERIMENTAL

Materials

The chemicals used in this study were ammonium heptamolybdate $[(\text{NH}_4)_6\text{Mo}_7\text{O}_{24} \cdot 4\text{H}_2\text{O}]$ (Prolabo high purity grade 99.97%) containing a maximum impurity (wt%) of Pb (0.001), Fe (0.001), Mg (0.02), Cl (0.001), NO_3 (0.02), and SiO_2 (0.0005). Ammonium paratungstate $[(\text{NH}_4)_{10}\text{H}_2\text{W}_{12}\text{O}_{42} \cdot 4\text{H}_2\text{O}]$ was prepared by Eurotungstène leading to a product with impurity contents of Mo (0.09 wt%), Fe (50 ppm), and SiO_2 (34 ppm).

Two methods have mainly been used for the synthesis of bulk mixed carbides. These, together with the designations of the materials, are described below.

Method 1. The first method, derived from metallurgical preparations, was based on the carburization of metals by carbon black at an elevated temperature (1520°C). The detailed procedure was as follows. A solution of hydrochloric acid (12 M) was added dropwise at room temperature under constant stirring to ammonium paratungstate and ammonium heptamolybdate solutions. After a reaction time of 6 hr at room temperature a coprecipitate of tungstic and molybdic acids was obtained. After thorough washing, the solid was filtered off under vacuum and dried in an oven at 110°C. The acid precipitates were then reduced at 860°C under flowing hydrogen to obtain a very fine metal powder of W and Mo (0.4- μm grain diameter). The carburization of the resulting metals was carried out by mixing with the stoichiometric amount of carbon (acetylene black) and reacting at 1520°C in order to obtain pure carbides according to phase diagram indications (9, 10). This method, used for the preparation of samples L643, A1, B1, C1, D1, and E1, led to very pure and well crystallized carbides, but because of the high temperature

of preparation, the surface areas were very low.

Method 2. The second method of preparation was at a lower temperature in order to try to obtain compounds with higher surface areas (samples CC). The reduction temperature of the mixed oxides under hydrogen was lowered to 600°C and then the carburization was performed under flowing carbon monoxide at 1000°C.

Other methods. Another method of preparation was used for sample L643-3. This was by chemical vapor deposition and is described in Ref. (7). Sample SII was provided by Telefunken without any information on the method of preparation.

Samples A1, B1, C1, D1, E1 have been prepared in collaboration with the laboratory of Ugicarb Morgon (France) while samples L643-1, L643-2, and CC have been obtained from Wimet (Great Britain), both subsidiary companies of Sandvik (Sweden). In addition, samples F and G were supplied by Battelle (Switzerland). They were synthesized according to Method 2 from raw materials provided by Sandvik.

After carburization, each sample was cooled to room temperature under flowing nitrogen and then subjected to a passivation treatment in a 2% O_2/N_2 stream prior to reduction or XPS experiments in order to avoid extensive oxidation during the transfer of solids in air.

Analytical Methods

The BET specific surface areas were determined by volumetric nitrogen adsorption performed with a Texas Instruments precision pressure gauge in a system already described elsewhere (11).

X-ray diffraction patterns of the samples were obtained using a Philips (Norelco PW 1051) apparatus ($\text{CuK}\alpha$ radiation $\lambda = 1.54178 \text{ \AA}$, Ni filter) at the Laboratoire de Cristallographie Minérale of the University of Poitiers.

XPS measurements were carried out with an AEI ES 200B spectrometer equipped with an Al anode ($h\nu = 1486.6 \text{ eV}$, 300 W).

In addition another spectrometer (Leybold-Heraeus, LHS 10) was used whenever ion etching was required. Two references were used for the calculation of binding energies (BE) (Au $4f_{7/2}$ = 84 eV and/or C $1s$ from *in situ* contamination = 285 eV).

Finally, molybdenum and tungsten contents were determined by atomic absorption spectrometry with $\lambda = 3132.6 \text{ \AA}$ for Mo and $\lambda = 2551 \text{ \AA}$ for W in a reducing flame of acetylene-nitrous oxide (N_2O). The metal amount determinations were carried out at the laboratory of Ugicarb Morgon (Grenoble) and at the Central Service of Chemical Analysis of the CNRS (Lyon).

The total amount of carbon was obtained from the combustion of the sample with oxygen in a high-frequency oven (LECO apparatus). Carbon dioxide was then quantitatively detected by a calibrated thermal conductivity cell with an oxygen reference flow which gave the percentage of carbon

directly. During the carburizing process the metal carbides were often loaded with free carbon, the quantity of which depends upon the preparation method. This free carbon content was obtained by coulometric measurements. The sample was attacked by a hot mixture of nitric and hydrofluoric acids which dissolved every component except for the noncombined carbon. Then, this remaining carbon was transformed into CO_2 by flowing oxygen at 1300°C ; the amount of CO_2 was determined with an electrochemical titration cell containing a barium perchlorate solution of known molarity.

RESULTS AND DISCUSSION

Bulk Compositions and BET

Surface Areas

Results are summarized in Table 1 for the samples prepared by Method 1 (see Experimental) and in Table 2 for those prepared by Method 2.

TABLE 1
Bulk Composition and Surface Areas of W, Mo Carbides

Samples ^a	Mo% ^b	W% ^c	Atom ratios			S (m ² g ⁻¹) ^g
			$\frac{\text{Mo}}{\text{Mo} + \text{W}}$ ^d	$\frac{\text{C}}{\text{Mo} + \text{W}}$ ^e	$\frac{\text{C}_F}{\text{Mo} + \text{W}}$ ^f	
WC						
CWF 2	0	93.89	0	0.992	0.005	1.3
L 643.1	0	93.90	0	0.998	0.005	1.4
L 643.2	0	93.83	0	0.999	0.016	2.4
L 643.3	0	94.15	0	0.935	0.016	2.8
(W, Mo) C						
A ₁	2.87	90.85	0.057	0.997	0.002	1.5
B ₁	9.54	83.66	0.179	0.988	0.028	1.2
C ₁	13.86	79.21	0.251	0.990	0.013	1.7
D ₁	14.65	78.42	0.264	0.996	0.001	0.4
Mo ₂ C						
E ₁	93.86	0	1	0.496	0.027	0.4

^a As prepared according to Method 1 by mixing acetylene black and metal powder (except L643.3).

^{b,c} Weight percent from atomic absorption flame spectrometry.

^d Atomic ratios.

^e Metal-carbon stoichiometry of mixed carbides or number of carbidic carbon atoms per metal atom.

^f Number of free carbon atoms over the total number of metal atoms.

^g BET surface areas.

TABLE 2
Bulk Composition and Surface Areas of Mo, W Carbides

Samples ^a	Mo% ^b	W% ^c	Atom ratios			S (m ² g ⁻¹) ^g
			$\frac{\text{Mo}}{\text{Mo} + \text{W}}$ ^d	$\frac{\text{C}}{\text{Mo} + \text{W}}$ ^e	$\frac{\text{C}_F}{\text{Mo} + \text{W}}$ ^f	
WC (Wimet)						
CC 1b-2	0	91.6	0	0.993	0.28	12.1
(W, Mo)C (Wimet)						
CC 2a-2	30.5	54.3	0.518	0.788	1.29	37.7
CC 2a-3	29.8	52.4	0.521	0.900	1.40	47.3
CC 3a-2	58.9	28.3	0.800	0.736	0.78	24.0
CC 2b-1	53.8	29.8	0.513	1.0	1.20	28.6
WC (Battelle)						
F	0	93.9	0	0.980	0.02	2.8
(W, Mo)C						
G (Battelle)	32.2	59.4	0.512	0.972	0.09	6
SII.1 (Telefunken)	30.6	60.5	0.492	0.810	0.42	34.8

^a As prepared according to Method 2 (carburization with CO) and additional samples from different industrial sources.

^{b,c} Weight percent from atomic absorption flame spectroscopy.

^d Atom ratios of the two metals.

^e Metal-carbon stoichiometry of carbides.

^f Number of free carbon atoms over the total number of metal atoms.

^g BET surface areas.

As expected from the first method of preparation using carburization with carbon at high temperature, the amount of free carbon is very low as shown in the sixth column of Table 1. Consequently the surface of the sample will be contaminated with carbon either not at all or very little. However, as a consequence of the high preparation temperature the specific surface areas of these samples are very low. As to the stoichiometry of the carbides, the ratio $C/(\text{Mo} + \text{W})$ (C is carbon inserted in the carbide) is close to unity for all the mixed carbides of Table 1, corresponding to the formula (Mo, W)C. In contrast, sample E₁ which contains no tungsten is represented by the formula Mo₂C.

The second method of preparation, by carburization with carbon monoxide at 1000°C, leads to solids with higher total surface areas but with larger proportions of free carbon as indicated by the values of the ratio $C_F/(\text{Mo} + \text{W})$ ranging between 0.28 and 1.4 (Table 2). Only samples F and G pre-

pared by Battelle contain less free carbon, but they also exhibit lower surface areas which makes these samples "hybrid" between the solids prepared via Methods 1 and 2. For all these samples, the total surface area increases with the amount of free carbon (Fig. 1). This observation unfortunately suggests that for solids of the series CC, the surface area is mainly developed by very small free carbon particles. Here, the ratio $C/(\text{Mo} + \text{W})$ (C is carbon inserted in the carbide) is generally lower than 1 (except for WC, samples CC 1b-2 and CC 2b-1) indicating a lack of carbidic carbon. It is not possible to assess whether such a lack is related to the higher proportions of Mo in the metal phase or to the procedure of preparation.

X-Ray Diffraction

Samples A, B, C, D, (Table 1). The published phase diagrams (9, 10) forecast that with our conditions of preparation for the

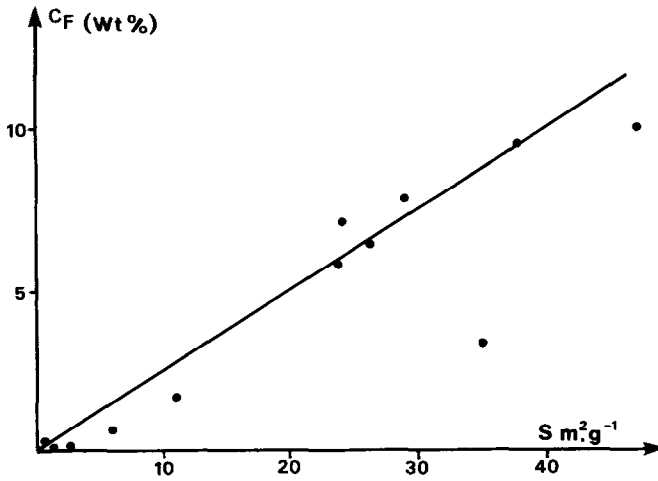


FIG. 1. Effect of the free carbon content (wt% C_F) on BET surface areas.

samples of this series, we should obtain mixed carbides (Mo, W)C with a simple hexagonal structure isotypic with WC for the compositions reported in Table 1 (11-15). This was also suggested by the chemical formulae corresponding to (Mo, W)C. In fact, X-ray diffraction patterns agree very well with these predictions. All the samples have a simple hexagonal structure, except for Mo₂C (E₁) which has a close-packed hexagonal structure (Fig. 2). The corresponding lattice constants are reported in Table 3. These constants were

computed from all the lines of the X-ray diffraction patterns using the equation

$$d_{hkl} = \frac{a}{[(4/3)(h^2 + k^2 + hk) + l^2a^2/c^2]^{1/2}}$$

characteristic of a hexagonal structure. As can be seen, the parameter c decreases with the relative atomic molybdenum percentage, as well as the ratio c/a .

The effect of treatment in hydrogen at 885°C for 12 h has been studied with the sample B₁. No structural change has been detected from the diffraction pattern, in

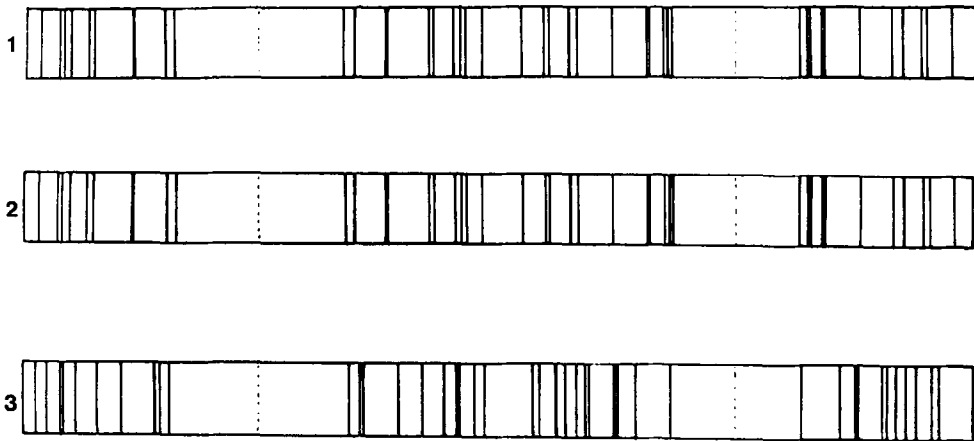


FIG. 2. X-ray diffraction patterns of W, Mo carbides. (1) WC (CWF2); (2) (Mo, W) C (B1); (3) Mo₂C (E₂).

TABLE 3

Lattice Parameters of Mo,W Mixed Bulk Carbides from XRD

Samples	$\frac{\text{Mo}}{\text{Mo} + \text{W}}$	<i>c</i> (nm)	<i>a</i> (nm)	<i>c/a</i>	<i>V</i> (pm) ³
WC					
L643.2	0	0.2834	0.2901	0.9768	20.655
(W, Mo)C					
A ₁	0.057	0.2834	0.2903	0.9760	20.683
B ₁	0.179	0.2830	0.2902	0.9751	20.640
C ₁	0.251	0.2830	0.2903	0.9749	20.654
D ₁	0.264	0.2824	0.2900	0.9732	20.568
G	0.512	0.2825	0.2903	0.9732	20.619
Mo ₂ C					
E ₁	1	0.4737	0.3011	1.573	18.596
Reference lattice constants					
α W ₂ C (Ref. (13))		0.4720	0.2990	1.578	
β Mo ₂ C (Ref. (14))		0.4729	0.3002	1.575	
WC (Ref. (15))		0.2830	0.2901	0.975	
γ MoC (Ref. (15))		0.2809	0.2898	0.969	

good agreement with the well-known thermal stability of such materials (see, for example, Ref. (31)).

From this X-ray diffraction study we conclude that these bulk carbides are perfect solid solutions where Mo is diluted in the WC lattice.

Samples CC and S (Table 2). At 1000°C, mixed phases (Mo, W)C can be obtained only for ratios $C/(\text{Mo} + \text{W}) \approx 1$ (10). For substoichiometric compounds (ratios $C/(\text{Mo} + \text{W}) < 1$) mixtures of phases isomorphous with WC (or hexagonal MoC) and W₂C (or hexagonal close-packed Mo₂C) are usually obtained (9–10).

X-ray diffraction experiments have been performed for two solids of this series: CC 3a-2 and SII-1. The diffraction patterns are rather ill-defined, with lines which are very broad and weak indicating that these solids are more amorphous than the solids of the first series, probably because of the higher amount of free carbon.

In Table 4 are summarized the main features of the patterns of CC 3a-2 and SII-1 together with those of the reference spectra of WC (25–1047), W₂C (2–1137), and Mo₂C (11–680) from JCPDS tables.

As shown in Table 4, these two catalysts have complex structures composed of mixtures of phases WC or MoC and W₂C or Mo₂C but with interplanar spacings slightly different. The spectra were too ill-defined

TABLE 4

X-Ray Data for Mixed W, Mo Carbides Using Debye-Scherrer Camera

CC 3a-2			S II-1			WC (25-1047) ^a			W ₂ C (2-1134) ^a			Mo ₂ C 11-680(27) ^a		
2θ	<i>d</i> (Å)	<i>I</i> ^b	2θ	<i>d</i> (Å)	<i>I</i>	<i>d</i> (Å)	<i>I</i>	<i>hkl</i>	<i>d</i> (Å)	<i>I</i>	<i>hkl</i>	<i>d</i> (Å)	<i>I</i>	<i>hkl</i>
32.15	2.78	W	31.95	2.80	VW	2.84	45	001						
34.60	2.59	VW							2.60	50	100	2.60	20	100
36.25	2.512	m	35.90	2.501	m	2.518	100	100						
37.40	2.404	W	37.05	2.426	W				2.36	40	002	2.37	30	002
39.55	2.278	VW							2.27	100	101	2.28	100	101
			47.65	1.908	VVW									
48.75	1.868	m	48.55	1.875	W	1.884	100	101						
									1.74	40	102	1.750	16	102
61.85	1.500	m	62.20	1.492	VVW				1.49	60	110	1.503	12	110
63.93	1.456	W	64.05	1.454	VVW	1.454	20	110						
						1.420	6	002						
									1.34	50	103	1.349	18	103
73.45	1.289	m	73.65	1.286	VW	1.2935	25	111	1.293	40	200	1.303	2	200
74.90	1.274	m	74.30	1.276	VVW	1.2586	14	200	1.26	50	112	1.269	16	112
												1.255	8	201

^a Reference X-ray Data from JCPDS tables.

^b W, weak; VW, very weak; m, medium.

TABLE 5
Mo $3d_{5/2}$ Binding Energy Reference Standards

Sample	Oxidation number	Binding energy (eV)	Calibration level	References
Mo	0	227.9	Fermi level	(17)
		228.1	C 1s = 285 eV	
MoO ₂	IV	230	C 1s = 285 eV	(18)
MoO _x	V	231.2	C 1s = 285 eV	(19, 20)
MoO ₃	VI	233.2	C 1s = 285 eV	(21)
Mo ₂ C	—	229	C 1s = 285 eV	Present study

to allow a computation of the lattice constants.

XPS

By XPS, we have studied the mixed carbides of Mo and W with low free carbon contents to determine their relative surface compositions. The reference binding energy values are reported in Tables 5 and 6 for W $4f_{7/2}$ and Mo $3d_{5/2}$. The differences in binding energies between W $4f_{7/2}$ and W $4f_{5/2}$ on the one hand and Mo $3d_{5/2}$ and Mo $3d_{3/2}$ on the other hand are constant and equal respectively to 2.1–2.2 and 3.1–3.2 eV. From the intensity ratios expressed as the ratios between the corresponding photopeak areas, we have calculated the average composition of the layer analyzed by XPS in the bulk catalysts (Table 7) by using the formula proposed by Ward *et al.* (27),

$$\frac{n_x}{n_y} = \frac{I_x}{I_y} \times \frac{\sigma_y}{\sigma_x} \times \left(\frac{E_y}{E_x}\right)^{1.7},$$

where I_x and I_y are the photopeak areas, σ are the cross sections ($\sigma(\text{W } 4f) = 9.8$, E are the kinetic energies corresponding to the levels under consideration, and $\sigma(\text{Mo } 3d) = 9.5$ from Ref. (30)). Then for each metallic element, W and Mo, we have estimated the proportion of oxide and of carbide phases using the following procedure. The W $4f_{7/2}$ and Mo $3d_{5/2}$ peaks of the carbidic species located at the right sides of the spectra (see Fig. 3 for example) are not greatly affected by the presence of oxides at higher binding energies. On the other hand, on pure compounds (single crystal MoO₃, WO₃, and metallic Mo or W) it can be shown that Mo $3d_{5/2}$ and W $4f_{7/2}$ peaks are almost perfectly symmetrical except for

TABLE 6
W $4f_{7/2}$ Binding Energy Reference Standards

Sample	Oxidation number	Binding energy (eV)	Calibration level	References
W	0	31.4	C 1s = 285 eV	(17)
		31.8	C 1s = 285 eV	(22)
		30.7	Au $4f_{7/2}$ = 83.8 eV	(26)
WO ₂	IV	33.5		(23)
		33.2	C 1s = 285 eV	(24)
WO ₃	VI	36.2	C 1s = 285 eV	(24)
		36		(22)
		36.4	Au $4f_{7/2}$ = 84 eV	(25)
WC	—	32.3	W $4f_{7/2}$ = 36.4 eV (WO ₃)	(25)
		32.2	C 1s = 285 eV	Present study

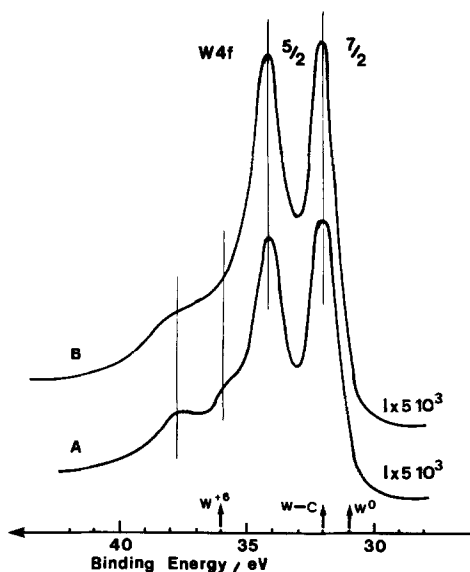


FIG. 3. W 4f XPS spectra of W, Mo mixed carbides (sample C₁). (A) Before argon etching; (B) after 12-min argon etching.

the presence of a small tail at the low kinetic energy side. Then the Mo 3d_{5/2} and W 4f_{7/2} peaks were considered symmetrical and their areas for the carbidic species were measured, and by taking into account the W 4f_{7/2-5/2} and Mo 3d_{5/2-3/2} intensity ratio, the total areas of the carbidic W 4f and Mo 3d doublets were estimated. Neglect of considering the tail could systematically underestimate the lower binding-energy peak areas by the order of a few percent. By difference with the total area under the broad feature W 4f or Mo 3d, the oxide contribution is deduced.

Catalysts after Passivation

As expected, since passivation consists in a superficial oxidation, W and Mo are in two phases: a carbide and an oxide (Figs. 3 and 4). Considering the distribution of W, in the mixed carbides, the proportion of oxide at the surface is roughly the same within the margin of experimental error (with an exception for sample G) and slightly lower than that for tungsten carbide. For Mo, if one excepts catalyst A₁ which contains a

very small proportion of molybdenum and for which the precision of the peak area measurements for Mo is consequently very low, the proportion of oxide is significantly higher than that for W. There remains the same exception as before for catalyst G.

Considering now the average proportions of Mo and of W in the layers analyzed by XPS, comparison of the last two columns of Table 7 indicates that the surface of mixed Mo, W carbides is enriched in molybdenum (except for sample G). Indeed, when the atom ratio Mo/(Mo + W) derived from XPS is plotted versus the bulk composition (Fig. 5) a straight line with a slope greater than unity is obtained. Such a molybdenum surface enrichment is in good agreement with the higher proportion of surface oxide for Mo than for W. This is probably even more important than suggested by this comparison since the ratio Mo/(Mo + W) calculated from XPS results is not for the uppermost layer only; this layer contributes not more than 10–20% to the signal measured.

In order to take this observation into consideration, we have tried to estimate the real Mo/(Mo + W) ratio at the surface by adapting the treatment of Van Langeveld and Ponc (16) for Auger electron spectroscopy.

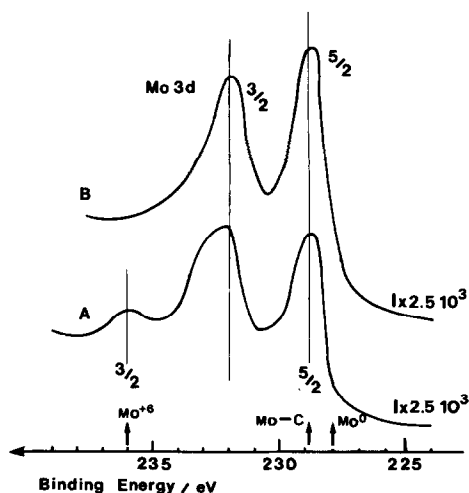


FIG. 4. Mo 3d XPS spectra of W, Mo mixed carbides (sample C₁). (A) Before argon etching; (B) after 12-min argon etching.

TABLE 7
Surface Composition of W, Mo Mixed Carbides from XPS Measurements after Passivation

Samples	W% ^d	W% ^e	Mo% ^f	Mo% ^g	Mo	Mo
	carbide	oxide	carbide	oxide	$\frac{\text{Mo}}{\text{Mo} + \text{W}}$ XPS % ^h	$\frac{\text{Mo}}{\text{Mo} + \text{W}}$ bulk % ⁱ
A ₁ ^a	69	31	74	26	7.5	5.7
b	66	34	87	13	5.7	—
B ₁ ^a	66	34	56	44	23.5	17.9
b	69	31	74	26	23.1	—
C ₁ ^a	62	38	53	47	34.7	25.1
b	66	34	63	37	33.8	—
D ₁ ^a	71	29	50	50	33.0	26.4
b	63	27	67	33	30.0	—
G ^a	58	42	58	42	52.3	51.2
c	59	41	66	34	51.3	—
L643-2	61	39				
	71	29				

^a From XPS spectra at zero time.
^b After 12 min of argon etching (3000 eV, 10 mA).
^c After 1 h of argon etching (3000 eV, 10 mA).
^{d-g} Atom percent of W or Mo phases in carbidic and oxidic forms.
^h Atom percent for surface composition from XPS experiments.
ⁱ Atom percent bulk composition from atomic absorption spectroscopy.

copy to XPS. Let us recall that in this model it is assumed that only the uppermost monolayer differs notably from the bulk composition. In an alloy AB the ratio

of the intensities of the signals of A and B can be written as

$$\left[\frac{I(A)}{I(B)} \right]_{\text{alloy}} = \frac{N_1^A x_1 + (1 - N_1^A) x_b}{N_1^B (1 - x_1) + (1 - N_1^B) (1 - x_b)} \times \frac{I_A}{I_B},$$

where I_A and I_B are the intensities of A and B signals corresponding to a single atom, N_1^A and N_1^B are the relative participations of the first monolayers of A and B to the intensity signals, while x_1 and x_2 are the atom fractions of A in the first monolayer and in the bulk of the alloy. As the surface enrichment is assumed to be restricted to the first monolayer,

$$N_1^A = \frac{I_1^A}{I(A)}$$

(I_1^A and $I(A)$ are respectively the intensities of the signal corresponding to the first monolayer and to the entire signal of A). Since the signal intensity of a layer situated

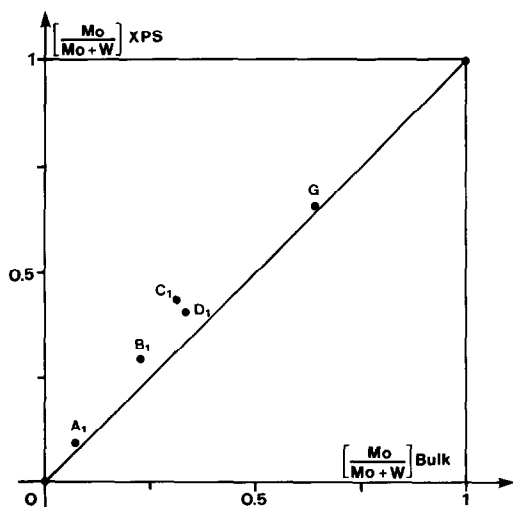


FIG. 5. Surface composition from XPS plotted as a function of bulk composition for mixed carbide catalysts.

TABLE 8

Bulk and Surface Composition of the Mo, W Mixed Carbide Catalysts

Samples	$\frac{\text{Mo}}{\text{Mo} + \text{W}}$ (atom ratio)			
	Bulk	Surface ^a		
		$N_1^b = 0.13$	$N_1 = 0.14$	$N_1 = 0.15$
A ₁	0.057	0.20	0.19	0.18
B ₁	0.179	0.61	0.58	0.585
C ₁	0.251	0.99	0.94	0.89
D ₁	0.269	0.78	0.74	0.71

^a As determined by XPS according to the Van Langeveld and Poncéc procedure (16).

^b Relative contribution of the first monolayer of Mo and W to the intensity signals.

at a distance d from the surface is $I = I_1 e^{-d/\lambda}$, the signal corresponding to the second monolayer will be $I_2 = I_1 e^{-c/\lambda}$, and for the i th monolayer $I_i = I_1 e^{-c(i-1)/\lambda}$. If one assumes that the distance c between two successive monolayers is equal to the diameter of an atom of the element, i.e., $c = 0.278$ and 0.282 nm respectively for Mo and W, then

$$N_1^A = \frac{I_1^A}{I_1^A \times \sum_{i=0}^{\infty} e^{-ic/\lambda}}$$

for an infinite crystal. λ , the free mean path, can be estimated according to Seah and Dench (28). For Mo, $\lambda = 1.82$ nm and for W, $\lambda = 1.96$ nm. Hence one can calculate $N_1 = 0.142$ and 0.134 respectively for pure molybdenum and pure tungsten.

Now for an alloy, or for a mixed carbide, N_1 for an element is not the same as that for the pure element. However, as N_1 is not very different for Mo and W, we have assumed that N_1 is 0.14 for both Mo and W in carbides in order to be able to estimate the surface compositions reported in Table 8.

If other assumptions are made for the estimation of c , the value of N_1 will differ slightly from 0.14. In order to have an idea of the variations of x_1 , we have calculated x_1 for three different values of N_1 , namely

0.13, 0.14, and 0.15. These calculations are necessarily rather inaccurate and one can wonder whether really for catalysts C₁ and D₁, which are quite similar, the difference for Mo/(Mo + W) is meaningful; it may be that this difference expresses only the uncertainty. Nevertheless, if these hypotheses are correct, the molybdenum surface enrichment is rather important.

Catalysts after Argon Etching (12 min, 3000 eV, 10 mA)

The previous results seem to be corroborated by the effects of a short argon etching on the XPS spectra of mixed carbides. Indeed this etching should act mainly on light elements such as O and C and have a relatively small effect on heavier elements such as Mo and W. The results show that the peaks of the Mo⁶⁺ surface oxide progressively decrease (Fig. 4) whereas the carbidic C peak increases and the C 1s peak from carbon contamination together with the O 1s peak decreases (Fig. 6), indicating that these elements are on the surface. Results in Table 7 show clearly that the argon etching induces an increase of the proportion of Mo atoms included in a carbide phase. In contrast, the relative proportion of W carbide and oxide (Fig. 3 and Table 7) hardly changes. These results are normal only if the proportion of W atoms at the

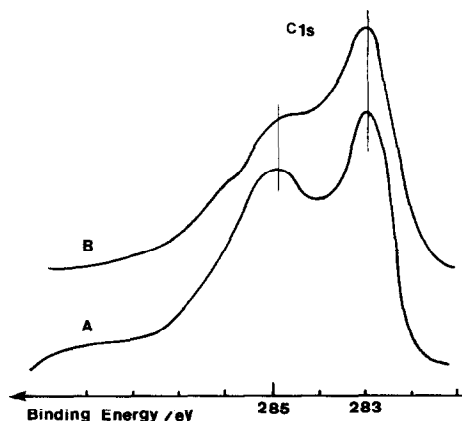


FIG. 6. C 1s XPS spectra of W, Mo mixed carbides (sample C₁). (A) Before argon etching; (B) after 12-min argon etching.

surface is lower than that in the inner layers.

Moreover, for WC alone (sample L643-2 in Table 7) after an argon etching of 8 min, the proportion of W carbide is more increased (61 to 71%) than that for the mixed carbides, indicating that the effects of etching, different on W and on Mo, are probably due to different surface distributions rather than to different behaviors of W and Mo.

In addition when considering the changes in the atomic ratios $\text{Mo}/(\text{Mo} + \text{W})_{\text{XPS}}$ after etching, one can see that, even though these changes are very small and of the order of magnitude of the experimental error, there is a very small systematic decrease of these ratios after etching, which could be due to partial removal of metal atoms of the uppermost layer. Indeed, if this layer is enriched with Mo and since the effect of etching is quite the same for Mo and W atoms, this would result in an increase of the $\text{Mo}/(\text{Mo} + \text{W})$ ratio, but of very low intensity since the efficiency of Ar etching is very low for these heavy metal atoms.

Hence all the XPS results give evidence of a surface composition modification. It is interesting to ask whether this surface enrichment is a result of the passivation treatment or if it preexisted in the catalyst. If it occurred during the oxidizing passivation treatment, one would expect a surface enrichment with the metal forming the highest energy bond with oxygen. Now the bond energies of Mo-O and W-O are respectively 115 and 156 kcal mol⁻¹, so in that case tungsten would be more likely to segregate at the surface than molybdenum. In contrast to this, the bond enthalpy is lower for molybdenum than for tungsten (28). Hence, because of the reduction in hydrogen at 860°C for all the bulk catalysts (except for sample G which was reduced at 600°C and for which no Mo surface enrichment was found), a surface enrichment in molybdenum after reduction could be expected. This Mo surface enrichment could also be explained by the differences in the melting temperatures of the trioxides

(MoO₃, 795°C; WO₃, 1473°C). The underlying unreduced MoO₃ could sublime (1155°C) and the mobility of this oxide could favor the molybdenum segregation to the surface during reduction or during carburization at 1520°C with carbon black. In this way, one could explain why in sample G which was reduced then carbided in carbon monoxide at lower temperature (600 to 1000°C) the molybdenum surface enrichment has not been found.

All this reasoning is in favor of a surface modification preexisting in the catalyst after its preparation, i.e., in the same state as that in which it will be tested in catalytic reactions.

Catalysts after Reduction in Hydrogen

Vidick *et al.* (29) have already shown that an activation treatment of 16 h at 300°C in a 50% H₂-in-Ar mixture almost completely reduced the surface of WC, oxidized during passivation. We have checked if this was also true for molybdenum carbide (sample E₁). Figure 7 gives the XPS signals for O 1s and Mo 3d after the passivating treatment (a) and after reduction in hydrogen for 3 h at 304°C (b) and for 13 h at 484°C (c). These reductions were performed in a reactor attached to the spectrometer via a dry N₂ purged glove box in order to avoid contamination of the sample with air. It is very clear that oxygen is progressively removed since the ratio $I_{\text{O}}/I_{\text{Mo}}$ of the intensities of O 1s and Mo 3d photopeaks decreased from 1.09 to 0.62 and 0.30. It should be noted that oxygen seems to be present in two forms, one giving a peak around 531.3 eV and another with a binding energy about 2 eV higher. After reduction, only the first peak at 531.3 eV BE is noticeably reduced. This peak probably corresponds to oxygen of passivation bound to Mo oxide. The origin of the second peak is not very clear but it could correspond to H₂O or to carbonate groups.

Similar results were obtained by reduction of a mixed Mo, W carbide (sample B1). In addition the ratio $n_{\text{Mo}}/n_{\text{W}}$ was not modi-

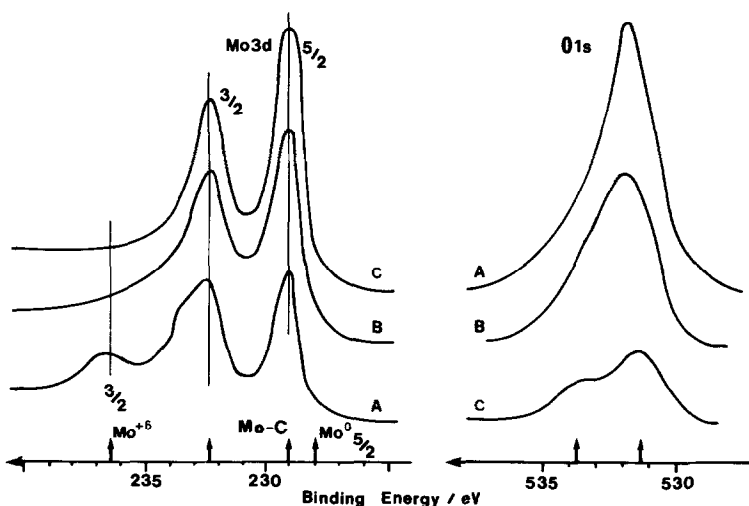


FIG. 7. Mo 3d and O 1s spectra of molybdenum carbide (sample E₁). (A) After the passivating treatment; (B) after reduction in hydrogen for 3 h at 304°C; (C) after reduction in hydrogen for 13 h at 484°C.

fied by reduction in flowing hydrogen at 500°C for 14 h showing that the surface composition of these catalysts after a reducing activation pretreatment (the one to which catalysts will be submitted before catalytic tests, see Part II) can be studied on passivated samples, thereby avoiding the time-consuming *in situ* pretreatment in the spectrometer.

CONCLUSIONS

Mixed bulk tungsten and molybdenum carbides have been prepared with a stoichiometry (C/(Mo + W)) close to 1 in order to be references for supported carbides which are less easy to characterize. These mixed carbides prepared at a high temperature (1520°C) are perfect solid solutions corresponding to a simple hexagonal structure isotypic with WC, at least in the range of compositions studied here (from 0 to 51 relative atom percent of Mo).

After preparation these catalysts must be transferred in air. For this reason they are passivated in low oxygen partial pressures which results in a surface oxidation of Mo and W. It has been shown that this oxygen of passivation can be removed by a further

reduction in hydrogen at temperatures of at least 400–500°C.

XPS analysis of passivated samples points to a molybdenum surface enrichment for the mixed W, Mo carbides. For all these carbides the atomic ratio Mo/(Mo + W) at the surface is about three times greater than the bulk ratio, if the surface composition is assumed to concern only the uppermost monolayer. Thermodynamic considerations indicate that such a surface enrichment is not a result of surface modifications occurring during the passivation treatment with low amounts of oxygen but that it occurs during the preparation of the carbides (reduction or carburization of the metals).

REFERENCES

1. Sinfelt, J. H., and Yates, D. J. C., *Nature (London) Phys. Sci.* **229**, 29 (1971).
2. Boudart, M., and Levy, R., *Science* **181**, 547 (1973).
3. Kojima, I., Miyazaki, E., Inoue, Y., and Yasumori, I., *J. Catal.* **59**, 472 (1979).
4. Boudart, M., Oyama, S. T., and Leclercq, L., in "Proceedings, 7th International Congress on Catalysis, Tokyo, 1980" (T. Seiyama and K. Tanabe, Eds.), Vol. 1, p. 578. Elsevier, Amsterdam, 1981.
5. Leclercq, L., in "Surface Properties and Catalysis

- by Non-metals" (J. P. Bonnelle, B. Delmon, and E. Derouane, Eds.), Nato A.S.I. Series C105, p. 433. Reidel, Dordrecht, 1983.
6. Kharlamov, A. I., *Kinet. Katal.* **21**, 1, 245 (1980).
 7. Leclercq, L., Imura, K., Yoshida, S., Barbee, T., and Boudart, M., in "Preparation of Catalysts II," *Stud. Surf. Sci. Catal.*, Vol. 3, p. 627. Elsevier, Amsterdam, 1979.
 8. Leary, K. J., Michaels, J. N., and Stacy, A. M., *J. Catal.* **101**, 301 (1986).
 9. Rudy, E., Kieffer, B., and Baroch, E., *Planseeber. Pulvermetall.* **26**, 105 (1978).
 10. Holleck, H., *Metall. (Berlin)* **3** (1981).
 11. Leclercq, G., and Boudart, M., *J. Catal.* **71**, 21 (1981).
 12. Anderson, J. R., "Structure of Metallic Catalysts." Academic Press, New York, 1975.
 13. Becker, Z. F., *Phys.* **51**, 481 (1928).
 14. Fries, R. J., Kempter, C. P., *Crystallogr. Data Anal. Chem.* **32**, 1898 (1960).
 15. Schonberg, N., *Acta Metall.* **2**, 427 (1954).
 16. Van Langeveld, A. D., and Ponc, V., *Appl. Surf. Sci.* **16**, 405 (1983).
 17. Fuggle, J. C., and Martensson, N., *J. Electron Spectrosc. Relat. Phenom.* **21**, 275 (1978).
 18. Dufresne, P., Grimblot, J., and Bonnelle, J. P., *Bull. Soc. Chim. France* **3**, 89 (1980).
 19. Kim, K. S., Baitinger, W. E., Amy, J. W., and Winograd, N., *J. Electron Spectrosc. Relat. Phenom.* **5**, 357 (1974).
 20. Cimino, A., and De Angelis, B. A., *J. Catal.* **36**, 11 (1975).
 21. Grimblot, J., Bonnelle, J. P., and Beaufile, J. P., *J. Electron Spectrosc. Relat. Phenom.* **8**, 437 (1976).
 22. Biloen, P., and Pott, G. T., *J. Catal.* **30**, 169 (1973).
 23. De Angelis, B. A., and Schiavello, M., *J. Solid State Chem.* **21**, 67 (1977).
 24. Vedrine, J. C., Hollinger, G., and Duc, T. M., *J. Phys. Chem.* **82**, 1515 (1978).
 25. Rodero, A., Ph.D. Thesis, University of South Florida, 1976.
 26. Ng, K. T., and Hercules, D. M., *J. Phys. Chem.* **80**, 2094 (1976).
 27. Ward, M. B., Lin, M. J., and Lunsford, J. H., *J. Catal.* **50**, 306 (1977).
 28. Seah, M. P., and Dench, W. A., *Surf. Interface Anal.* **1**, 83 (1979).
 29. Vidick, B., Lemaitre, J., and Delmon, B., *J. Catal.* **99**, 428 (1986).
 30. Scofield, J. H., *J. Electron Spectrosc. Relat. Phenom.* **8**, 129 (1976).
 31. Toth, L. E., "Transition Metal Carbides and Nitrides," p. 4. Academic Press, New York, 1971.